The Cryosphere Discuss., 7, 1383–1414, 2013
www.the-cryosphere-discuss.net/7/1383/2013/
doi:10.5194/tcd-7-1383-2013

The Cryosphere Discussions
Open Access

Discussion Paper | Discussion Paper | Discussion Paper | Discussion Paper |

A decade of supraglacial lake volume estimates across a land-terminating margin of the Greenland Ice Sheet

A. A. W. Fitzpatrick[1], **A. L. Hubbard**[1], **J. E. Box**[2], **D. J. Quincey**[3], **D. van As**[2], **A. P. B. Mikkelsen**[4], **S. H. Doyle**[1], **C. F. Dow**[5], **B. Hasholt**[4], **and G. A. Jones**[1]

[1]Institute of Geography and Earth Sciences, Aberystwyth University, Aberystwyth, UK
[2]Geological Survey of Denmark and Greenland (GEUS), Copenhagen, Denmark
[3]School of Geography, University of Leeds, Leeds, LS2 9JT, UK
[4]Department of Geography and Geology, University of Copenhagen, Denmark
[5]Glaciology Group, College of Science, Swansea University, Swansea, SA2 8PP, UK

Received: 15 February 2013 – Accepted: 27 February 2013 – Published: 3 April 2013

Correspondence to: A. A. W. Fitzpatrick (aaf07@aber.ac.uk)

Published by Copernicus Publications on behalf of the European Geosciences Union.

Abstract

Supraglacial lakes represent an ephemeral storage buffer for runoff and lead to significant, yet short-lived, episodes of ice-flow acceleration by decanting large fluxes of meltwater and energy into the ice sheet's hydrological system. Here, a field-validated methodology for calculating lake volume is used to quantify storage and drainage across Russell Glacier catchment, west Greenland, from 2002 onwards. Using 502 optical satellite images, water volume at ∼ 200 seasonally occurring lakes was derived from a *depth-reflectance* relationship, independently calibrated and field-validated against lake bathymetry. Inland expansion of lakes is strongly correlated with air temperature: during the record melt years of 2010 and 2012, lakes formed and drained earlier, attaining their maximum volume 38 and 20 days before the 11 yr mean, as well as occupying a greater area and forming at higher elevations (> 1800 m) than previously. Although lakes occupy only 2 % of the catchment surface area, they temporarily store up to 13 % of the bulk meltwater discharged. Across Russell Glacier, 28 % of supraglacial lakes drain rapidly and clustering of such events in space and time suggests a synoptic trigger-mechanism. Furthermore, we find no evidence to support a unifying critical size or depth-dependent drainage threshold hypothesis.

1 Introduction

Meltwater runoff from the Greenland Ice Sheet (GrIS) has increased since the 1960s (Hanna et al., 2005) and has been linked to seasonal ice-flow variability through basal hydrological forcing (Zwally et al., 2002; Joughin et al., 2008; van de Wal et al., 2008; Bartholomew et al., 2010). Horizontal and vertical ice surface motion lags peak daily melt and responds to rapid supraglacial lake (SGL) tapping (Shepherd et al., 2009; Das et al., 2008; Doyle et al., 2013). Furthermore, the spatial pattern of seasonal flow acceleration coincides with the development of ice sheet surface hydrology (Palmer et al., 2011; Fitzpatrick et al., 2013) where SGLs play a vital role via temporary storage and routing of surface meltwater. SGLs, which are prevalent across the entire GrIS (Selmes et al., 2011) also drain rapidly via hydraulic fracture propagation in ~ 2 h (Das et al., 2008; Doyle et al., 2013), forming moulins that provide a direct hydraulic connection to the ice sheet bed. Previous studies on SGLs have quantified spatial and temporal variations in SGL area across different sectors of the GrIS (e.g. Georgiou et al., 2009; Sundal et al., 2009; Selmes et al., 2011; Liang et al., 2012), and have estimated their volume (e.g. Box and Ski, 2007; Sneed and Hamilton, 2007), whilst others have attempted to model SGL evolution (e.g. Luthje et al., 2006; Banwell et al., 2012) and measure bed melt rate (Tedesco et al., 2012a). The extent to which temperatures correlate with melt volume and SGL storage remains unclear, and critically, for modelling studies the existence of a volumetric threshold exists beyond which rapid SGL drainage is inevitable.

We investigate the seasonal evolution of SGLs over RGC using 11 yr (2002–2012) of lake volume estimates. This period includes a number of extremely warm years when melt records were exceeded (Nghiem et al., 2012; Tedesco et al., 2012b), and therefore provides an opportunity to determine how the life cycle of SGLs are modulated by regional climatic forcing. The year 2010 was the warmest on record (Cappelen et al., 2012; Box et al., 2010), 2.5 standard deviations above the 1973–2010 average in west Greenland (van As et al., 2012). Temperatures for April, June and July in 2012 also rank amongst the warmest on record (Cappelen et al., 2012), resulting in the second warmest summer (after 2010) and the largest spatial extent of melt on record (Nghiem et al., 2012). We present a field calibrated algorithm for calculating changes in SGL volume during these years and compare them with longer-term patterns derived over the period 2002–2012.

2 Study area

Russell Glacier Catchment (RGC) is an ideal region to investigate SGL dynamics as this sector of the GrIS accounts for the highest areal extent of SGLs across the ice-sheet (Selmes et al., 2011). This study covers ~ 6500 km^2 of the west GrIS between 66.8 and 67.3° N and extends from the ice margin to ~ 2000 m elevation (~ 150 km inland, Fig. 1). For hydrological impact assessment, this catchment benefits from a long term meteorological record obtained from a transect of six automated weather stations extending well above the local equilibrium line altitude to 1830 m (van As et al., 2012; van de Wal et al., 2012) and bulk proglacial discharge gauged at Watson River, Kangerlussuaq since 2007 (Hasholt et al., 2012).

3 Methods

3.1 Calculating lake extent

SGL areas were calculated using multitemporal Moderate Resolution Imaging Spectroradiometer (MODIS) imagery from the Terra satellite. We used the level 2, MOD09 product, which provides ungridded swaths of atmospherically corrected, calibrated and geolocated surface reflectance. MRTSwath version 2.2 (https://lpdaac.usgs.gov/tools) was used to convert the atmospherically corrected MOD09 land product from HDF swath format to a geographically referenced gridded image using the corresponding MODIS level 1B 1 km geolocation file for each image (MOD03). Although the region experiences 24-h daylight in summer, illumination conditions alter with changing solar zenith angle, therefore scenes used in this study were restricted to those captured at nadir. Scenes covering the entire melt-season were obtained from 2002 to 2012 from day of year (DOY) 121 (1 May) to DOY 274 (30 September).

Given the size of RGC we opted for a semi-automatic strategy to classify SGL extents, using the Normalized Difference Water Index (Huggel et al., 2002, Eq. 1) and freely available RSGISlib software (http://www.rsgislib.org). Before classification, MODIS bands within the visible spectrum (0.46 to 0.67 µm; bands 3 and 4) were sharpened from 500 m to 250 m resolution, using the ratio of bands 1 and 2 (at 250 m and 500 m resolution, respectively, L. Gumley et al., http://earthdata.nasa.gov/sites/default/

TCD
7, 1383–1414, 2013

files/field/document/MODIS_True_Color.pdf). The approach for identifying water cover was to isolate regions with a high reflectance in the blue spectral band (band 3), utilizing their striking colour contrast against the surrounding ice. Thresholds for both red and blue bands were used in combination with the NDWI threshold to reduce misclassification of pixels with spectrally similar signals to SGLs. A cloud filter was also included in the classification using MODIS band 6, which is sensitive to solid and liquid phase water, and final SGL classification was subsequently carried out on pixels which had band 6 reflectance of less than 0.15 consistent with Box and Ski (2007).

$$\mathrm{NDWI} = \frac{(b3 - b1)}{(b3 + b1)} \tag{1}$$

3.2 Depth and volume estimation

SGL volume was calculated using an empirically derived depth-reflectance relationship. To derive this relationship we surveyed the bathymetry of two SGLs in July 2010, referred to here as Lake F (67.00° N, 48.71° W) and Lake Z (66.96° N, 48.78° W). On 26 June 2010, Lake F was instrumented with water level sensors and on 29 June the lake perimeter was surveyed using a Leica System 500 Global Positioning System (GPS) receiver differentially corrected against a bedrock-mounted reference station. Following lake drainage on 30 June (Doyle et al., 2013), six elevation transects were surveyed over the lake bed. The combination of lake bathymetry and depth time series allowed for shoreline reconstruction (Doyle et al., 2013). The second, undrained lake was surveyed by mounting a depth sounder (Garmin X10) and GPS receiver (Leica System 500) on an inflatable raft, whilst the perimeter was surveyed using a similar GPS setup.

The depth sounder has a stated accuracy of ±0.1 m. The GPS transect data and the extrapolated margins for both lakes were interpolated onto a 10 × 10 m grid using kriging interpolation to yield lake bathymetry maps (Fig. 2). Lake perimeter measurements were overlaid onto MODIS imagery from corresponding days. MODIS pixels that contained more than 50 % water were accepted as lake pixels, constraining the minimum and maximum band thresholds for water. SGL bathymetries (Fig. 2) were interpolated to 250 m resolution to match the MODIS band 1 resolution, so that data could be extracted and plotted to reveal the relationship between depth and surface reflectance (Fig. 3a). Following Box and Ski (2007), the relationship between depth and surface reflectance can be approximated by a least-squares fit, where D is depth and R is MODIS band 1 reflectance:

$$D = \frac{0.65}{(0.035 + R)} - 0.4 \quad (2)$$

Equation 2 was then applied to all water classified pixels across the study region to yield depth estimates and were subsequently integrated over the SGL area to calculate water volume.

3.3 Uncertainty estimation

3.3.1 Area

We evaluated the accuracy of the classification by comparing the area of individual SGLs extracted from MODIS data with a SGL area dataset derived from finer spatial resolution (15 m) panchromatic LANDSAT ETM+ images. In total, 62 lakes (free of surface ice) were manually digitized from four panchromatic LANDSAT ETM+ images from different years and at different stages of the melt season (26 June 2008, 17 July 2004, 20 July 2005, 8 August 2006). The comparison shows a strong agreement between the two data sets (Fig. 3b) with strong correlation ($r^2 = 0.97$) and a root-mean-square deviation (RMSD) of 0.14 km^2, comparable with previous studies (e.g. 0.11 km^2, Selmes et al., 2011, and 0.22 km^2, Sundal et al., 2009). This RMSD value was multiplied by the number of SGLs occurring each day to provide error margins for total SGL area estimates.

The minimum area of any individual SGL identified from MODIS images is restricted by pixel size (0.0625 km^2) thereby introducing potential bias in total lake area and its size distribution. Previous work using higher resolution products calculated that small lakes ($< 0.1\,km^2$) account for 12 % of the total lake area based on analysis of a single mid-season ASTER image (Sundal et al., 2009). In our study SGLs smaller than $0.0625\,km^2$ were identified from a LANDSAT ETM+ image (26 June 2008), indicating that they account for 7.5% of the total SGL area at this time. From the same image, 11.1 % of SGLs were found to be smaller than $0.1\,km^2$ in line with the Sundal et al. (2009) study.

3.3.2 Volume

Depth surveys were undertaken on two SGLs located to the north of the study area on 14 and 15 July 2005, referred to as lakes A and B in Box and Ski (2007), and on lake Disco on 22 July and 8–9 August 2007. The results of these four surveys were overlaid onto the corresponding MODIS derived depth maps enabling comparison (Fig. 3c). There is good agreement between MODIS-derived depth and actual depth ($r^2 = 0.79$, RMSD value of 1.47 m). To calculate percent volumetric error, the point measurements from the Disco surveys were gridded and interpolated onto a 10 m grid, with the lake margin delimited from a Landsat 7 image acquired on the 8 August 2007. The $9.5 \times 10^{-3}\,km^3$ calculated SGL volume agrees within 15 % of the volume from MODIS from 22 July ($11.3 \times 10^{-3}\,km^3$) and 8–9 August ($11 \times 10^{-3}\,km^3$) 2007.

3.4 Limitations

A key limitation to tracking SGL evolution is the temporal and spatial continuity of available imagery. Cloud cover in MODIS imagery reduces the temporal coverage of data, preventing every-day monitoring of SGLs, therefore missing the formation and drainage of some SGLs.

Consideration should also be given to the accuracy of the volume calculation, which relies on the calibration lake depths being representative of the whole SGL population, as deeper lakes may exist elsewhere on the ice sheet. The maximum depth a SGL can attain is limited by surface topography and slope and it is unlikely that much deeper lakes exist than are described here or in previous work (Box and Ski, 2007).

Finally the depth-reflection function itself limits the accuracy of the volume results as it relies on accurate calculations of atmospherically corrected surface reflection and reliable bathymetry measurements. Previous remote sensing studies (e.g. Liang et al., 2012) have presented lake area estimates which, although more reliable to attain, are not as representative of lake dynamics or contribution to the ice sheets water budget as volume estimates.

4 Results

Our aggregate dataset reveals that an average of 200 SGLs (> 0.0625 km^2) are observed each year within the 6500 km^2 RGC (Fig. 1). However, this total number varies year to year (Fig. 7a) with a standard deviation of ±20 lakes of which 21 % have persisted throughout the study period. Lakes have, on average, an area of 0.68 km^2 but can grow as large as 8.2 km^2 (66.92° N, 48.15° W). SGLs formed 21 days earlier in 2010 compared to the 11 yr mean, with small lakes forming at low elevations by 9 May (Fig. 4 and Table 1). The maximum total volume of SGLs at any one time from 2002 occurred on 23 June 2012 (DOY 175) when over 0.25 km^3 of water was stored across the surface of RGC coincident with the warmest month in four decades. The largest individual SGL volume was 0.038 km^2 on 14 July 2011 (DOY 195), during the second warmest July on record.

Intra-annually, the timing of lake formation, periods of peak storage and lake drainage events are highly variable, but it is clear from cumulative plots of lake volume that during high melt years (2010 and 2012), formation and drainage occurs much earlier in the season than in comparatively low melt years (e.g. 2002 and 2006; Fig. 6a). The mean maximum extent of lakes between 2002 and 2012 at each 200 m elevation interval illustrates that smaller lakes tend to form at lower elevations (< 1000 m) than larger lakes (Fig. 6b). There is also large annual variability in the percentage of rapidly

TCD
7, 1383–1414, 2013

draining lakes (defined here as those tapping within a 4-day period), with 28 % of lakes classified as such since 2002 (Fig. 7e). There is no obvious correlation with overall melt, although the peak number of rapidly tapping lakes did occur in the peak melt year (2012). However, in record warm years, characterized by a greater number of cloud free MODIS images, then it is possible that a bias is introduced and that the greater number of rapid draining SGLs identified is a consequence of more images being available. In all years, SGLs tend to form and drain at progressively higher elevations throughout the melt season consistent with previous studies (e.g. McMillan et al., 2007; Liang et al., 2012; Doyle et al., 2013). Using 2010 as an example (Fig. 8a), lakes can be seen storing and draining meltwater within five elevation bands. During 2010, 83 % of SGL volume was lost from those located between 1000 and 1600 m (Fig. 8b) with only 9 % and 7 % of water lost from lakes under 1000 m and above 1600 m, respectively.

Although lakes generally form in the same locations each year, there is significant inter-annual variability in the maximum areal extent of SGLs within each 200 m elevation band (Fig. 9a). The maximum areal extent of lakes during high temperature summers was: 158 km^2 in 2003; 154 km^2 in 2007; 136 km^2 in 2010; 160 km^2 in 2011 and 160 km^2 in 2012 (Cappelen et al., 2012); significantly larger than in other years. For example, SGL maximum areal extent was 40 % greater in the record melt year of 2012 compared with the low melt year of 2006. Furthermore, during 2012 lakes occupied a larger area (49 %) above 1400 m (96.6 km^2) than in previous years (11-yr average of 64.7 km^2) (Fig. 9a). The years 2003 and 2007 gave the second and third highest elevation lake extents above 1400 m a.s.l., 33 % and 25 % greater than the 11 yr mean, respectively. The maximum areal extent of lakes above 1400 m for each year in the period 2002-2012 was compared with mean monthly temperatures of June and July (Cappelen et al., 2012), revealing a positive correlation (r^2 = 0.78) supporting findings of SGLs forming at higher elevations in the highest temperature years (Fig. 9b). With the exception of the cooler years of 2002 and 2006, there is a significant temporal trend in both lake volume loss and the maximum elevation of lakes over the last decade (Fig. 7d, f).

TCD
7, 1383–1414, 2013

Seasonal patterns of SGL meltwater storage closely correlate with melt rates derived from an energy balance model (van As et al., 2012) for 2009/10 when data are available (Fig. 4). Peaks in surface meltwater runoff and storage in lakes generally precede increases in discharge recorded from the Watson River (van As et al., 2012; Hasholt et al., 2012). Volume lost from lakes was compared to peaks in the river discharge record to determine if specific SGL drainage events can be identified (Fig. 5). Our results indicate that SGL drainage does coincide with short-term perturbations in Watson River discharge, providing tentative evidence for the impact of changing supraglacial water storage on catchment-wide hydrology.

Lake drainage maps (Fig. 10) illustrate the seasonal lake evolution, highlighting the spatial and temporal variations of rapidly (< 4 days) draining and slow (> 4 days) draining lakes between years. SGLs in the Russell catchment generally tend to fit the same drainage pattern each year, remaining rapid or slow draining and not switching between years. There is no relationship between lake size (volume/area) and its mode of drainage. In some areas of RGC, SGLs were observed to drain in clusters, i.e. lakes within close proximity were observed to drain on the same day or within a few days of each other (Fig. 11), potentially impacting on the proglacial discharge hydrograph (Fig. 5).

5 Discussion

5.1 Inland expansion of supraglacial lakes

Using a field-calibrated and independently validated depth-reflectance function we track the area and volume of 200 ± 20 individual SGLs from 2002 until present across RGC (Figs. 1, 7a and 10). The recurrence of SGLs in the same positions each year (Fig. 1) is in agreement with previous work (Thomsen et al., 1988; Echelmeyer et al., 1991) and indicates that they do not advect down-glacier with ice flow. Lampkin and Vanderberg (2011) and Sergienko (2013) demonstrated that ice surface topography is strongly linked to the underlying basal topography, reinforcing the idea that SGLs form above the same subglacial basins each year. Within our study area, the persistent SGLs (21 % of the population) are preferentially located away from the fast-flow units as identified by Palmer et al. (2011).

The largest lake area observed within the study area was 8.25 km^2, coinciding with a maximum volume of 0.038 km^3, comparable to findings by Box and Ski (2007). On average, the maximum volume of any single lake (Lv_{max}) occurs on 25 July (DOY 206), ~ 12 days after the regional maximum volume (Tv_{max}) (Table 1; Fig. 4) because larger lakes tend to form at higher elevations, later in the season and also take longer to fill (Fig. 6b). The total number of SGLs within any year shows no relationship with Tv_{max} and Lv_{max} (Fig. 7b, c). For example in 2012, 200 lakes were observed, however Tv_{max} was 80 % greater than the 11-yr mean, and SGLs formed at higher elevation than in all previous years (Fig. 7d). Lake size varies with elevation, smaller lakes form at low (< 1000 m a.s.l.) and high elevations (> 1600 m a.s.l.), with the largest lakes forming in between (Fig. 6b). The majority (84 % in 2010) of water stored in lakes occurs within the 1000–1600 m elevation band (Fig. 8b), reflecting the effect of ice sheet hypsometry on lake morphology. The steeper slopes and crevassing associated with fast-flow at lower elevations within this region (Palmer et al., 2011; Fitzpatrick et al., 2013) prevents lakes from growing too large before drainage occurs. At higher elevations above 1600 m, lower temperatures and the shorter season limits meltwater availability and lake growth. However, SGL expansion in this upper melt zone is extremely sensitive to positive temperature and melt anomalies and may be used to track long-term climate trends (Howat et al., 2013).

Availability of surface runoff, governed in turn by surface temperatures and winter snow-pack, determines the initiation of lake formation (Fig. 4, Johansson et al., 2013). The timing and duration of individual lake drainage events varies inter-annually (Fig. 10), explaining the large differences between the total volume of water stored in lakes in each year (Fig. 4). During recent record warm years (2010 and 2012) SGLs formed earlier and attained their Tv_{max} on DOY 156 and DOY 174, 38 and 20 days earlier than the 11-yr mean, respectively (Fig. 4 and Table 1). The record melt of 2010 was exceeded in 2012 during which the largest melt extent within the satellite era (~ 97 % of the ice sheet) was observed (Nghiem et al., 2012). During 2012, melt lasted up to two months longer than the 1979–2011 mean (Tedesco et al., 2012b), and although we record no increase in the number of lakes (Fig. 7a), the total volume of SGL, Tv_{max} was ~ 80 % greater than the 11-yr mean and lakes were observed at higher elevations (> 1800 m) and occupied a greater area (> 1400 m) than in previous years (Figs. 7b, d and 9a, b).

Lake drainage events have contributed directly to hydrograph anomalies in the discharge record from Watson River. For example, the rapid drainage of a number of large SGLs between DOY 175–184 (24 July–3 August) during 2010 (Fig. 5, Doyle et al., 2013) coincided with a peak in discharge without a corresponding peak in melt (Fig. 5). Our data reveals considerable inter-annual variations in water storage and loss (Figs. 4 and 6a), with no two years following the same pattern. The rapid formation and drainage of lakes during the record melt year of 2012 strongly contrasts with the slow formation of lakes during the relatively cool year of 2006 (Fig. 6a). Assuming that all lakes within the study area encompassing RGC drain via the Watson River, a comparison between cumulative volume loss and discharge reveals that lakes temporarily store and release on average 13 % of total discharge (Table 2).

Under a future warming climate (Meehl et al., 2007), SGLs are expected to expand further into the ice-sheet interior as melt-season extent and duration increase. We present evidence supporting previous work (Liang et al., 2012; Howat et al., 2013), illustrating that in higher temperature years SGLs formed at higher elevations (Figs. 7d and 9b). The regression function of this study suggests a 1°C summer warming above the 2002–2012 mean would increase the elevation of lake formation to 1780 m. Lakes occupied a significantly larger area at higher elevations (> 1400) during 2012 (Fig. 9a) than in previous years (49 % greater than the 11 yr average). This coincides with the highest mean June/July temperatures recorded in Kangerlussuaq (Fig. 9b) and the greatest Greenland melt extent on record (Nghiem et al., 2012). Furthermore, we find a positive relationship between the maximum areal extent of lakes above 1400 m a.s.l. and mean monthly temperatures of June and July (Fig. 9b). Solar radiation absorption of SGLs, causes expansion of their existing basins (Box and Ski, 2007; Tedesco et al., 2012a), creating a positive albedo-feedback allowing SGLs to reform in successive years provided sufficient meltwater. Despite the high melt season of 2010, the maximum extent of SGLs above 1400 m only matched the 11-yr mean (Fig. 9a). However, during 2010, SGLs in each of the lower elevation bands were larger than all other years (Fig. 6b), indicating that the large volume of melt in 2010 primarily occurred across lower elevations. A similar pattern occurred in the warm summer of 2003, where SGLs occupied a below average extent above 1600 m (Fig. 9a), but the average maximum lake size between 1400–1600 m was 60 % greater than 11-yr mean (Fig. 6b).

5.2 Rapid lake drainage events

Rapid SGL drainage events are known to provide a mechanism for surface waters to penetrate through km-thick ice establishing hydraulic pathways through which meltwater continues to drain through the remainder of the melt season (Das et al., 2008; Doyle et al., 2013). Over the 11 yr of this study, on average 28 % of the SGL population underwent rapid drainage (Figs. 7e and 10). As the number of SGLs occurring higher up-glacier increases (Figs. 7d and 9a), more will rapidly drain, potentially expanding the region affected by melt-induced accelerated flow. We also note that at higher elevations, a number of SGLs appear to double drain in higher melt years. For example, in 2012 a 5.2 km^2 SGL located at 1400 m drained completely on the 23/24 June, subsequently refilled and by the 5 July had completely drained again. Such observations indicate that the subglacial hydrological system may not readily adapt to surface meltwater inputs as has recently been postulated (e.g. Sundal et al., 2011) and that basal hydrostatic creep-closure rates across the upper ablation zone where ice thickness is greater than 1 km exceed those processes which help to maintain an efficient hydrological system for the remainder of the season (Schoof, 2010).

Spatial and temporal clustering of SGL drainage events (Figs. 10 and 11) provides evidence that neighboring SGLs dynamically trigger synoptic-scale tapping. Previous work postulates that a lake containing 0.0983 km^3 of water, upon drainage and without being laterally constrained will spread over a subglacial area of 97 km^2 assuming a void thickness of 1 m (Box and Ski, 2007). We suggest that the drainage of neighbouring SGLs act to mechanically trigger one another via short-term perturbations in the regional stress/strain regime. Significant surface rifts and fractures are visible in SGLs that have been directly observed to drain rapidly (Das et al., 2008; Doyle et al., 2013), and are the primary mode of drainage identified in these studies. Many SGLs drain in this manner each year and there appears to be no common critical threshold of lake volume or depth which appears to control drainage initiation. We infer that the rapid drainage trigger mechanism is likely site-specific, governed by the seasonal routing and delivery of meltwater moderated by the regional stress/strain distribution and inherent mechanical resilience of the locality.

6 Conclusions

Using 502 cloud-free atmospherically corrected MODIS images we derived water volumes from ~ 200 seasonally occurring SGLs between 2002 and 2012 using a simple field-calibrated and validated depth-reflectance relationship. Although SGLs in our study occupy a relatively small area of the catchment (2 %), they store a disproportionate volume of bulk runoff (13 %) and have important implications for ice dynamics through the release of surface meltwater into the subglacial hydrological system via rapid in situ drainage or through overflow into moulins. We find evidence of SGLs draining in clusters, potentially impacting on bulk discharge gauged at Watson River, and infer that one drainage event dynamically triggers rapid tapping in neighbouring lakes. We find that lake size does not influence its drainage mechanism, and that there is no evidence for a critical lake depth or volume threshold to initiate rapid drainage.

In years of high summer temperatures, SGLs form and drain earlier in the season (e.g. 38 and 20 days earlier than the 11 year mean during 2010 and 2012, respectively), and cover a larger surface area (e.g. 40 % greater in the record melt year of 2012 compared with the cooler year of 2006). Furthermore, inland expansion of SGLs is strongly correlated with air temperature ($r^2 = 0.78$), with lakes occupying a greater area within the upper ablation zone. For example, in 2012, lake area was 49 % greater above 1400 m compared with the 11 yr mean) and extending further inland (> 1800 m) than previously recorded. In a warming climate, spatial and temporal expansion of SGLs with concomitant surface to bed coupling will likely impact on inland ice sheet flow dynamics and drawdown.

Acknowledgements. This research was funded by UK Natural Environmental Research Council grant NE/G005796 and the Greenland Analogue Project (Sub-project A). We also acknowledge startup support from the Aberystwyth University Research Fund, The Royal Geographical Society and the Gilchrist Trust without which this study would not have been initiated. MODIS data are distributed by the Land Processes Distributed Active Archive Center (LP DAAC), located at the USGS EROS Center (lpdaac.usgs.gov). Jeffrey Schmaltz is thanked for advice on MODIS data processing. Landsat data are distributed by the US Geological Survey (glovis.usgs.gov). AF kindly acknowledges a combined NERC/AU studentship bursary.

References

Banwell, A., Arnold, N., Willis, I., Tedesco, M., and Ahlstrøm, A.: Modeling supraglacial water routing and lake filling on the Greenland Ice Sheet, J. Geophys. Res., 117, F04012, doi:10.1029/2012JF002393, 2012. 1385

Bartholomew, I., Nienow, P., Mair, D., Hubbard, A., King, M., and Sole, A.: Seasonal evolution of subglacial drainage and acceleration in a Greenland outlet glacier, Nat. Geosci., 3, 408–411, doi:10.1038/NGEO863, 2010. 1384

Box, J. and Ski, K.: Remote sounding of Greenland supraglacial melt lakes: implications for subglacial hydraulics, J. Glaciol., 53, 257–265, doi:10.3189/172756507782202883, 2007. 1385, 1387, 1388, 1389, 1390, 1393, 1395, 1396

Box, J., Cappelen, J., Decker, D., Fettweis, X., Mote, T., Tedesco, M., and van de Wal, R. S. W.: Greenland, in: Arctic Report Card 2010, edited by: Richer-Menge, J., 55–64, 2010. 1385

Cappelen, J., Laursen, E., Kern-Hansen, C., Boas, L., Wang, P., Jørgensen, B., and Carstensen, L.: Weather and Climate Data from Greenland 1958–2011, in: Technical Report 12-15, Danish Meterological Institute, Copenhagen, 2012. 1385, 1391

Das, S., Joughin, I., Behn, M., Howat, I., King, M., Lizarralde, D., and Bhatia, M.: Fracture propagation to the base of the Greenland ice sheet during supraglacial lake drainage, Science, 320, 778–781, doi:10.1126/science.1153360, 2008. 1384, 1385, 1395, 1396

Doyle, S. H., Hubbard, A. L., Dow, C. F., Jones, G. A., Fitzpatrick, A., Gusmeroli, A., Kulessa, B., Lindback, K., Pettersson, R., and Box, J. E.: Ice tectonic deformation during the rapid in situ drainage of a supraglacial lake on the Greenland Ice Sheet, The Cryosphere, 7, 129–140, doi:10.5194/tc-7-129-2013, 2013. 1384, 1385, 1387, 1391, 1394, 1395, 1396

Echelmeyer, K., Clarke, T., and Harrison, W.: Surficial glaciology of Jakobshavns Isbrae, West Greenland, J. Glaciol., 37, 368–382, 1991. 1392

Fitzpatrick, A., Hubbard, A., Joughin, I., Quincey, D., van As, D., Mikkelsen, A., Doyle, S., Hasholt, B., and Jones, G.: Ice flow dynamics and surface meltwater flux at a land-terminating sector of the Greenland Ice Sheet, J. Glaciol., accepted, 2013. 1384, 1393

Georgiou, S., Shepherd, A., McMillan, M., and Nienow, P.: Seasonal evolution of surpaglacial lake volume from ASTER imagery, Ann. Glaciol., 50, 95–100, 2009. 1385

Hanna, E., Huybrechts, I., Janssens, J., Cappelen, K., Steffen, K., and Stephens, A.: Runoff and mass balance of the Greenland ice sheet: 1958–2003, J. Geophys. Res.-Atmos., 110, D13108, doi: 10.1029/2004JD005641, 2005. 1384

Hasholt, B., Mikkelsen, A., Nielsen, M., and Larsen, M.: Observations of runoff and sediment and dissolved loads from the Greenland ice sheet at Kangerlussuaq, West Greenland, 2007 to 2010, Z. Geomorphol., doi:10.1127/0372-8854/2012/00121, 2012. 1386, 1392

Howat, I. M., de la Peña, S., van Angelen, J. H., Lenaerts, J. T. M., and van den Broeke, M. R.: *Brief Communication* "Expansion of meltwater lakes on the Greenland Ice Sheet", The Cryosphere, 7, 201–204, doi:10.5194/tc-7-201-2013, 2013. 1393, 1394

Huggel, C., Kaab, A., Haeberli, W., Teysseire, P., and Paul, F.: Remote sensing based assessment of hazards from glacier lake outbursts: a case study in the Swiss Alps, Canad. Geotech. J., 39, 316–330, 2002. 1386

Johansson, A., Jansson, P., and Brown, I.: Spatial and temporal variations in lakes on the Greenland Ice Sheet, J. Hydrol., 476, 314–320, 2013. 1393

Joughin, I., Das, S., King, M., Smith, B., Howat, I., and Moon, T.: Seasonal speedup along the western flank of the Greenland Ice Sheet, Science, 320, 781–783, doi:10.1126/science.1153288, 2008. 1384

Lampkin, D. J. and Vanderberg, J.: A preliminary investigation of the influence of basal and surface topography on supraglacial lake distribution near Jakobshavn Isbræ, Hydrol. Process., 25, 3347–3355, doi:10.1002/hyp.8170, 2011. 1392

Liang, Y., Colgan, W., Qin, L., Steffen, K., Abdalati, W., Stroeve, J., Gallaherb, D., and Bayoub, N.: A decadal investigation of supraglacial lakes in West Greenland using a fully automatic detection and tracking algorithm, Remote Sensing Environ., 123, 127–138, 2012. 1385, 1390, 1391, 1394

Luthje, M., Pedersen, L., Reeh, N., and Greuell, W.: Modelling the evolution of supraglacial lakes on the West Greenland ice-sheet margin, J. Glaciol., 52, 608–618, 2006. 1385

McMillan, M., Nienow, P., Shepherd, A., Benham, T., and Sole, A.: Seasonal evolution of supraglacial lakes on the Greenland Ice Sheet, Earth Planet. Sci. Lett., 262, 484–492, 2007. 1391

Meehl, G., Stocker, T., Collins, W., Friedlingstein, P., Gaye, A., Gregory, J., Kitoh, A., Knutti, R., Murphy, J., Noda, A., Raper, S., Watterson, I., Weaver, A., and Zhao, Z.: Global climate projections, in: Climate Change 2007: The Physical Science Basis, Contribution of Working Group I to the Fourth Assessment Report of the Intergovernmental Panel on Climate Change, Cambridge University Press, Cambridge, UK and New York, NY, USA, 2007. 1394

Nghiem, S. V., Hall, D. K., Mote, T. L., Tedesco, M., Albert, M. R., Keegan, K., Shuman, C. A., DiGirolamo, N. E., and Neuman, G.: The extreme melt across the Greenland Ice Sheet in 2012, Geophys. Res. Lett., 39, 1–6, doi:10.1029/2012GL053611, 2012. 1385, 1394

Palmer, S., Shepherd, A., Nienow, P., and Joughin, I.: Seasonal speedup of the Greenland Ice Sheet linked to routing of surface water, Earth Planet. Sci. Lett., 302, 423–428, doi:10.1016/j.epsl.2010.12.037, 2011. 1384, 1393

Schoof, C.: Ice-sheet acceleration driven by melt supply variability, Nature, 468, 803–806, doi:10.1038/nature09618, 2010. 1395

Selmes, N., Murray, T., and James, T. D.: Fast draining lakes on the Greenland Ice Sheet, Geophys. Res. Lett., 38, L15501, doi:10.1029/2011GL047872, 2011. 1385, 1386, 1388

Sergienko, O.: Glaciological twins: basally controlled subglacial and supraglacial lakes, J. Glaciol., 59, 3–8, 2013. 1392

Shepherd, A., Hubbard, A., Nienow, P., King, M., McMillan, M., and Joughin, I.: Greenland ice sheet motion coupled with daily melting in late summer, Geophys. Res. Lett., 36, L01501, doi:10.1029/2008GL035758, 2009. 1384

Sneed, W. and Hamilton, G.: Evolution of melt pond volume of the surface of the Greenland Ice Sheet, Geophys. Res. Lett., 34, L03501, doi:10.1029/2006GL028697, 2007. 1385

Sundal, A., Shepherd, A., Nienow, P., Hanna, E., Palmer, S., and Huybrechts, P.: Evolution of supra-glacial lakes across the Greenland Ice Sheet, Remote Sensing Environ., 113, 2164–2171, doi:10.1016/j.rse.2009.05.018, 2009. 1385, 1388, 1389

Sundal, A., Shepherd, A., Nienow, P., Hanna, E., Palmer, S., and Huybrechts, P.: Melt-induced speed-up of Greenland ice sheet offset by efficient subglacial drainage, Nature, 469, 521–524, doi:10.1038/nature09740, 2011. 1395

Tedesco, M., Lüthje, M., Steffen, K., Steiner, N., Fettweis, X., Willis, I., Bayou, N., and Banwell, A.: Measurement and modeling of ablation of the bottom of supraglacial lakes in western Greenland, Geophys. Res. Lett., 39, L02502, doi:10.1029/2011GL049882, 2012a. 1385, 1395

Tedesco, M., Fettweis, X., Mote, T., Wahr, J., Alexander, P., Box, J., and Wouters, B.: Evidence and analysis of 2012 Greenland records from spaceborne observations, a regional climate model and reanalysis data, The Cryosphere Discuss., 6, 4939–4976, doi:10.5194/tcd-6-4939-2012, 2012b. 1385, 1394

Thomsen, H., Thorning, L., and Braithwaite, R. J.: Glacier-hydrological conditions on the Inland Ice north-east of Jakobshavn/Ilulissat, West Greenland, Rapport Grønlands Geologiske Undersøgelse, 138, Cophenhagen, Denmark, 1988. 1392

van As, D., Hubbard, A. L., Hasholt, B., Mikkelsen, A. B., van den Broeke, M. R., and Fausto, R. S.: Large surface meltwater discharge from the Kangerlussuaq sector of the Greenland ice sheet during the record-warm year 2010 explained by detailed energy balance observations, The Cryosphere, 6, 199–209, doi:10.5194/tc-6-199-2012, 2012. 1385, 1386, 1392

van de Wal, R. S. W., Boot, W., van den Broeke, M. R., Smeets, C. J. P. P., Reijmer, C. H., Donker, J. J. A., and Oerlemans, J.: Large and rapid melt-induced velocity changes in the ablation zone of the Greenland Ice Sheet, Science, 321, 111–113, doi:10.1126/science.1158540, 2008. 1384 van de Wal, R., Boot, W., Smeets, C., Snellen, H., van den Broeke, M., and Oerlemans, J.: Twenty-one years of mass balance observations along the k-transect, West Greenland, Earth Sys. Sci. Data, 4, 31–35, 2012. 1386

Zwally, H., Abdalati, W., Herring, T., Larson, K., Saba, J., and Steffen, K.: Surface melt-induced acceleration of Greenland ice-sheet flow, Science, 297, 218–22, doi:10.1126/science.1072708, 2002. 1384

TCD

7, 1383–1414, 2013

A decade of supraglacial lake volume estimates

A. A. W. Fitzpatrick et al.

Table 1. The date and day of year of maximum total lake volume (Tv_{max}) across the study region and maximum individual lake volume (Lv_{max}) between 2002 and 2012. The day the first SGL was observed, the number of days SGL were present and the elevation of the highest SGL (> 0.1 km^2) is also given.

Year	Day of Tv_{max}	Date of Tv_{max}	Tv_{max} (km^3)	Day of Lv_{max}	Date of Lv_{max}	Lv_{max} (km^3)	Day of first SGL	Number of days SGLs present	Highest SGL (> 0.1 km^2) elevation
2002	192	11 Jul	0.1369	192	11 Jul	0.0184	157	108	1661
2003	199	18 Jul	0.1496	203	22 Jul	0.0281	151	108	1660
2004	199	17 Jul	0.109	237	24 Aug	0.0231	151	90	1698
2005	207	26 Jul	0.144	217	5 Aug	0.0305	155	80	1706
2006	206	25 Jul	0.0958	236	24 Aug	0.0155	131	125	1652
2007	193	12 Jul	0.1844	191	10 Jul	0.0297	165	84	1757
2008	221	8 Aug	0.1451	221	8 Aug	0.0273	148	96	1697
2009	196	15 Jul	0.0938	197	16 Jul	0.0112	154	98	1689
2010	156	5 Jun	0.0896	192	11 Jul	0.0241	129	138	1790
2011	195	14 Jul	0.1546	195	14 Jul	0.038	159	87	1827
2012	174	22 Jun	0.2522	187	5 Jul	0.024	150	103	1826
Mean	194	13 Jul	0.142	206	25 Jul	0.0245	150	102	1724

TCD
7, 1383–1414, 2013

Table 2. The contribution of lake volume to discharge from the Watson River assuming all lakes within RGC drain through this outlet.

Year	Discharge (km^3)	Lake vol lost (km^3)	Lake contribution (%)
2007	3.67	0.4967	13.5
2008	2.86	0.5376	18.8
2009	2.57	0.3219	12.5
2010	5.46	0.4588	8.4
Mean			13.3

TCD
7, 1383–1414, 2013

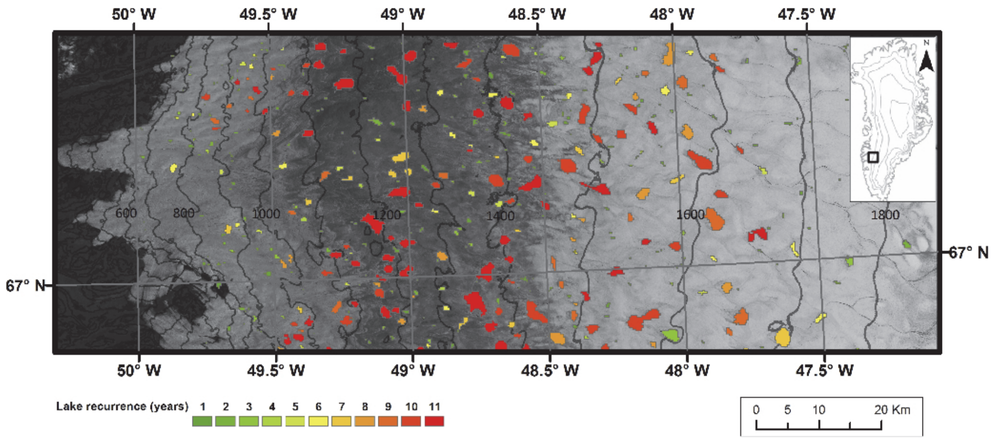

Fig. 1. The location of all the SGL's within the study area between 2002–2012, coloured by their recurrence.

TCD
7, 1383–1414, 2013

A decade of supraglacial lake volume estimates

A. A. W. Fitzpatrick et al.

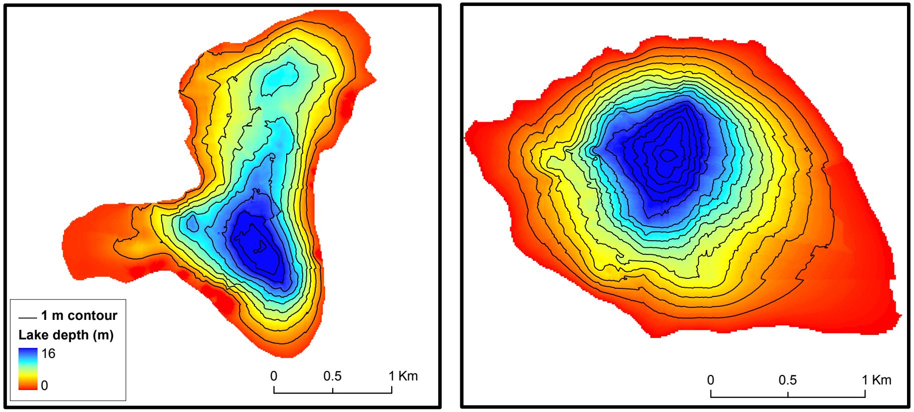

Fig. 2. Bathymetry maps of lake F and lake Z, data from which was used to calibrate the depth-reflectance curve.

TCD
7, 1383–1414, 2013

A decade of supraglacial lake volume estimates

A. A. W. Fitzpatrick et al.

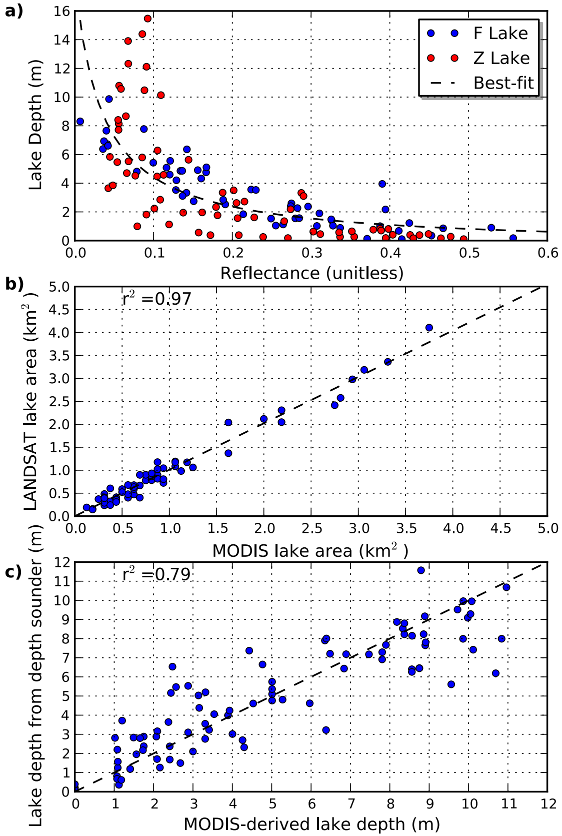

Fig. 3. (a) Lake F and Z MODIS band 1 reflectance vs. depth with best fit curve; **(b)** the relationship between lake area estimates derived from manually digitising 15 m resolution panchromatic LANDSAT 7 images and the automated MODIS classification; and **(c)** the relationship between independently measured lake depth for 3 SGLs and modelled lake depth using the MODIS depth-reflectance relationship.

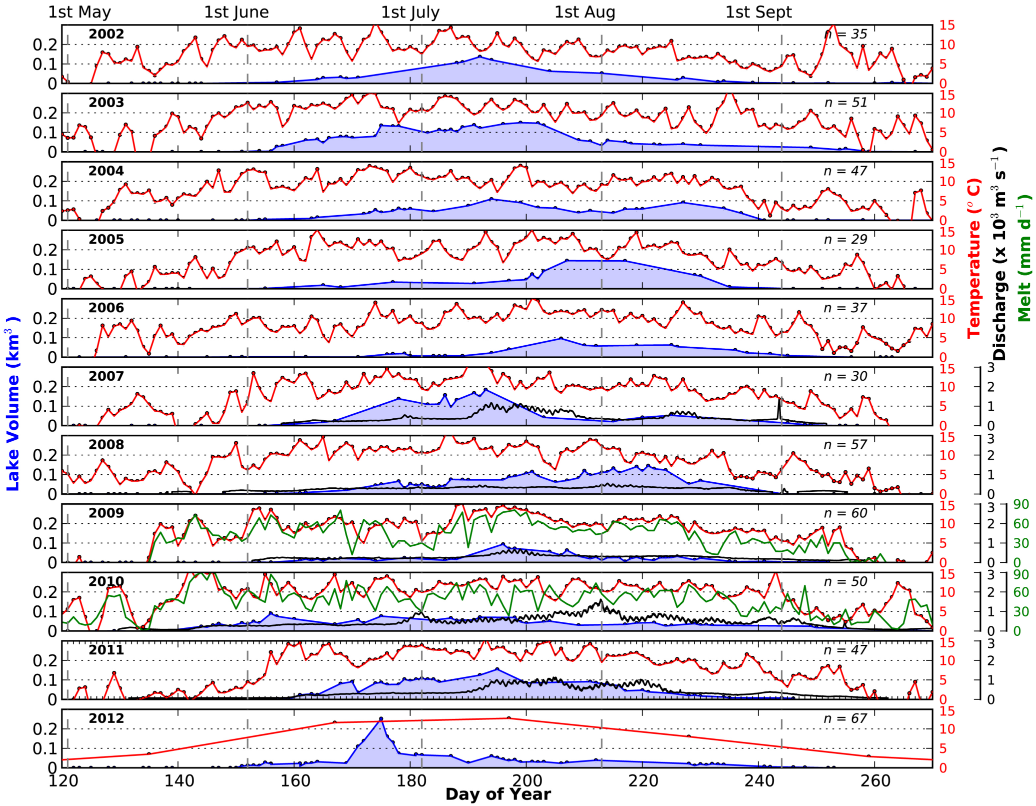

Fig. 4. Total lake volume within Russell Glacier catchment (blue), Kangerlussuaq air temperature (red), surface melt (green) and proglacial Watson River discharge (black) between 2002–2012. Only monthly average air temperature data is currently available for 2012. Surface melt rate and Watson River discharge are only shown for years when data are available. The number of cloud-free observations of SGLs (denoted *n*) per year is given.

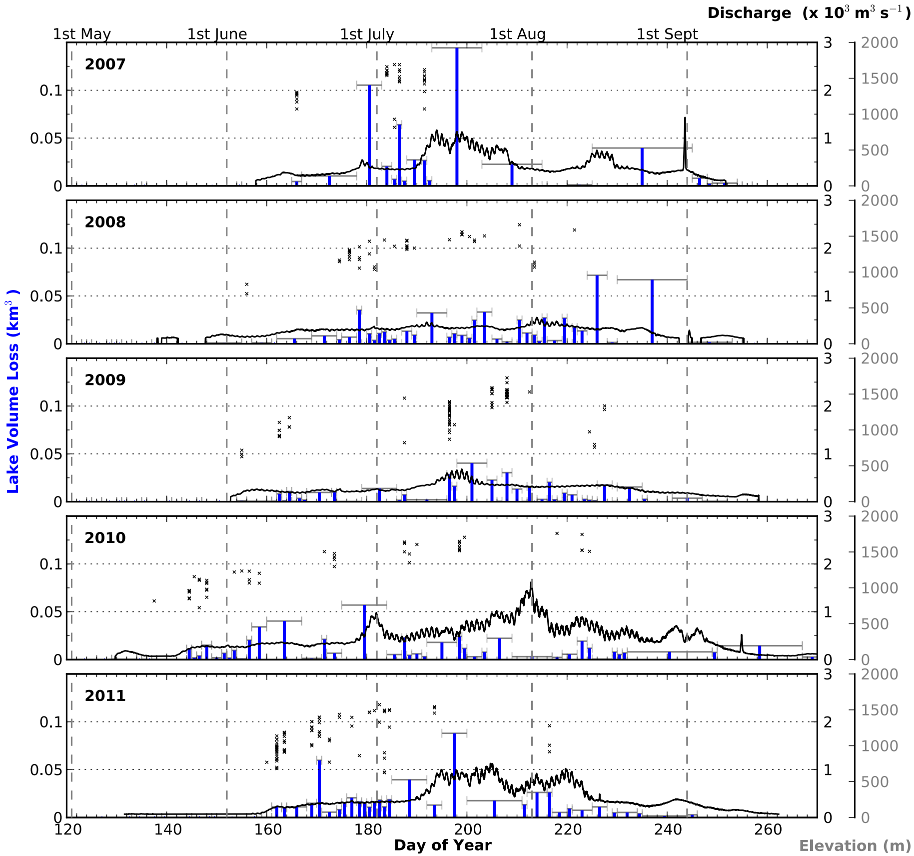

Fig. 5. Lake volume loss within RGC and Watson River discharge between 2007 and 2011. The drainage date and elevation of rapidly draining SGLs are also shown (black crosses).

TCD
7, 1383–1414, 2013

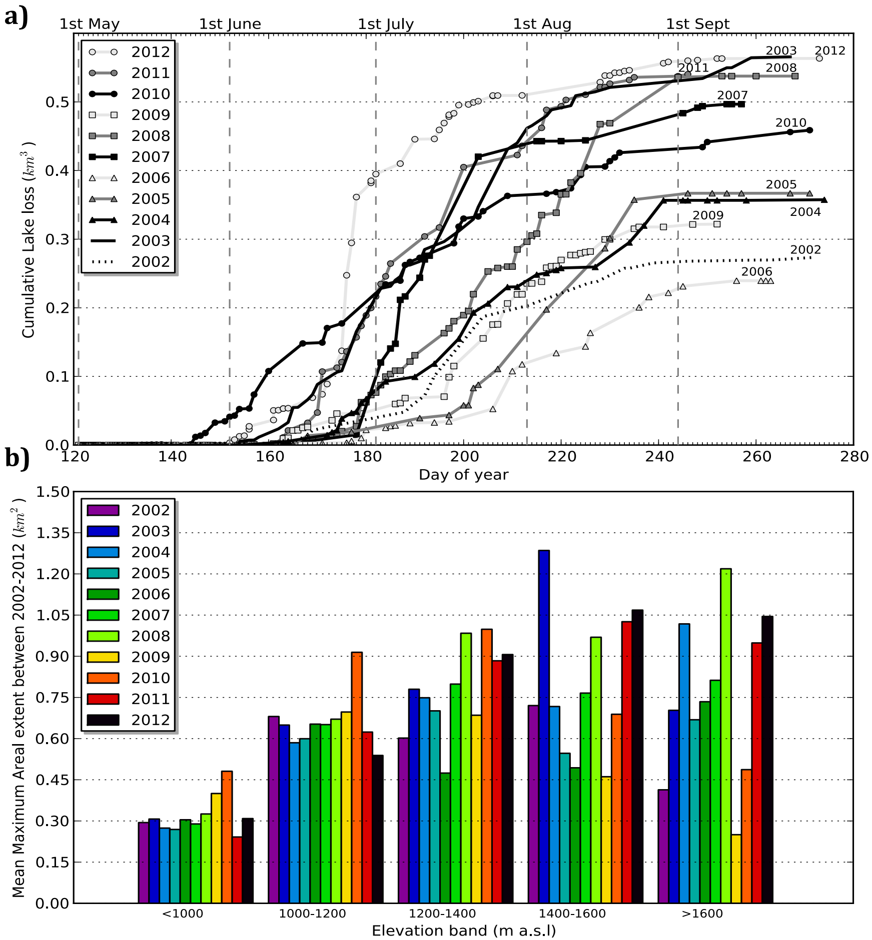

Fig. 6. (a) Cumulative lake volume loss within Russell Glacier catchment and **(b)** mean areal extent of SGL's binned at 200 m elevation intervals between 2002–2012.

TCD

7, 1383–1414, 2013

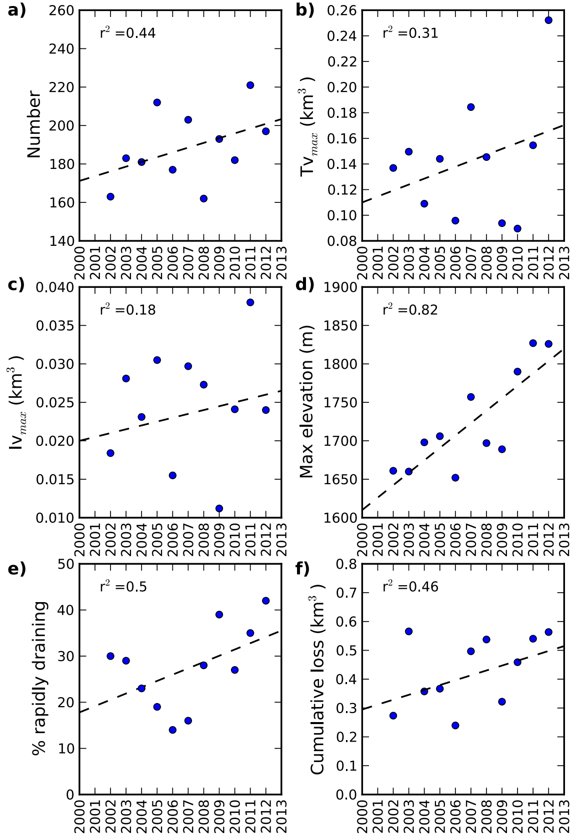

Fig. 7. Inter-annual differences in lake characteristics including **(a)** lake number, **(b)** regional maximum lake volume (Tv_{max}), **(c)** individual SGL volume (Lv_{max}), **(d)** maximum SGL elevation, **(e)** percentage of rapidly draining SGLs and **(f)** cumulative SGL volume loss.

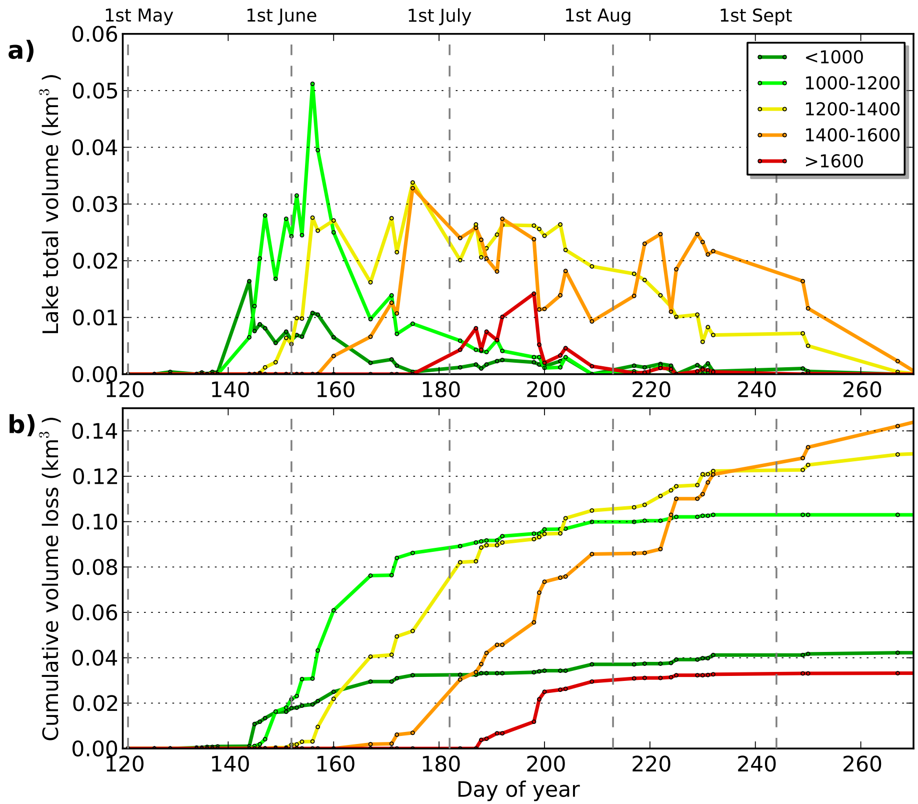

Fig. 8. (a) Total lake volume and **(b)** cumulative lake volume loss at 200 m elevation bands during 2010.

TCD
7, 1383–1414, 2013

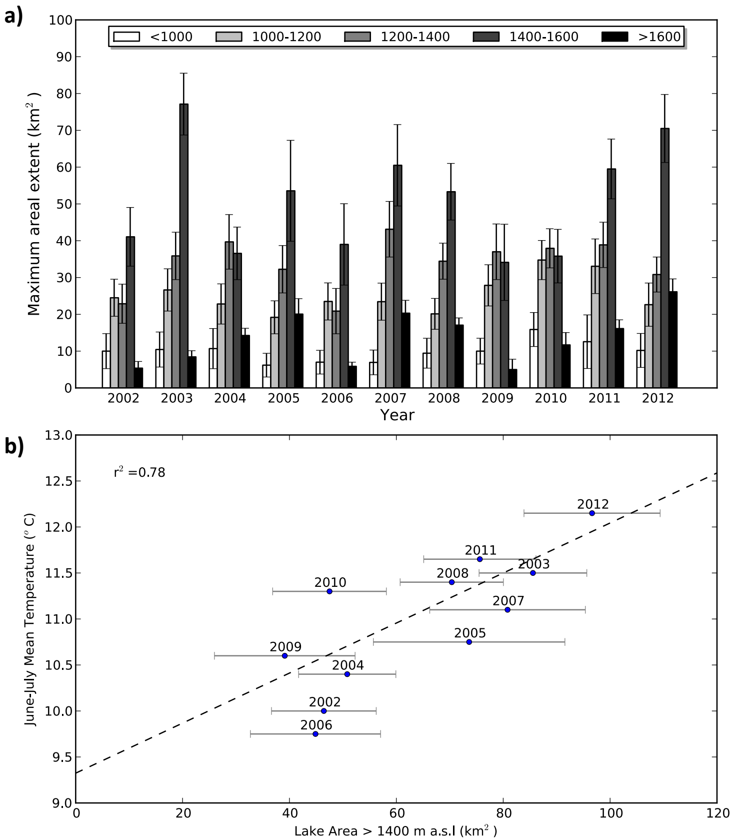

Fig. 9. (a) Maximum areal extent of SGLs within each 200 m elevation band and **(b)** the relationship between maximum areal extent of SGLs above 1400 m and mean peak summer temperatures (June/July) between 2002–2012.

TCD
7, 1383–1414, 2013

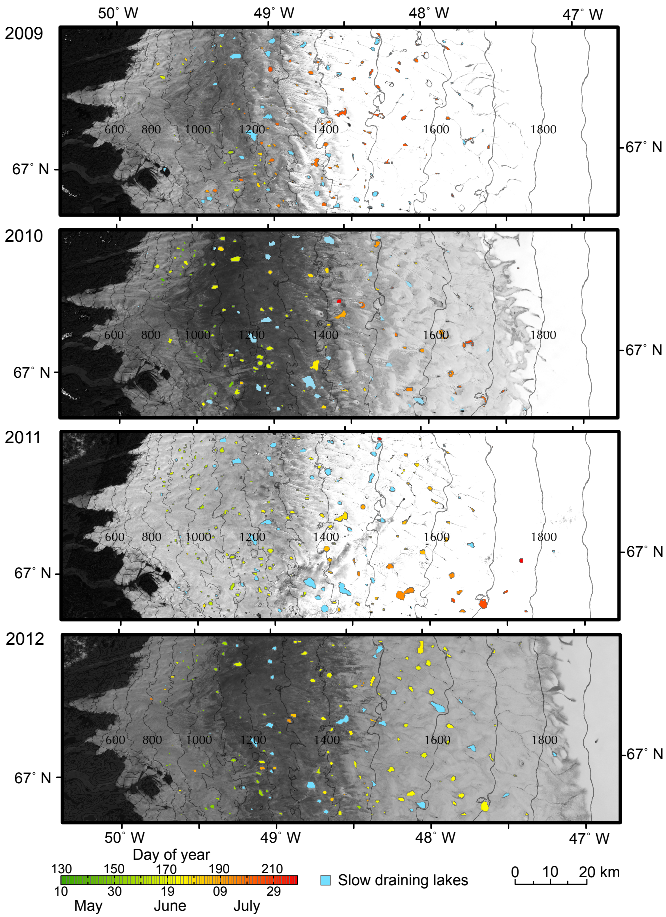

Fig. 10. Colour coded lake drainage maps during 2009–2012 highlighting the inter-annual variability of lake drainage. Background images are Landsat 7 from, 31 July 2009, 19 August 2010, 28 June 2011 and 16 July 2012.

TCD
7, 1383–1414, 2013

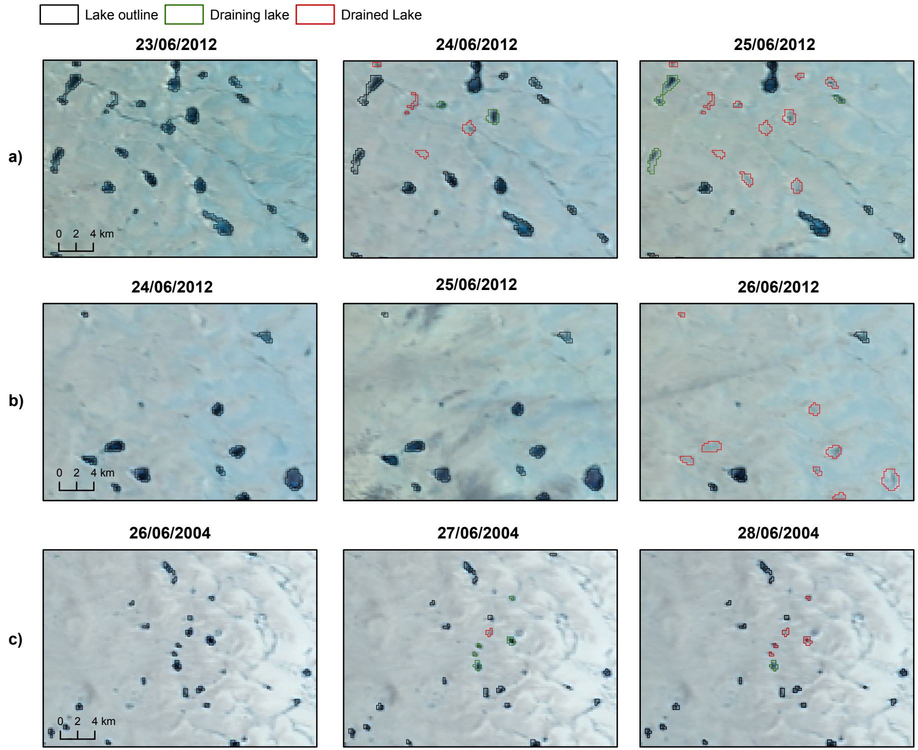

Fig. 11. Clustering of SGL drainage events in three different regions of our study area during **(a)** June 2012 and **(b)** June 2012 and **(c)** June 2004. SGL outlines from the first day are shown in black, SGLs in the process of draining and those that have drained are shown in green and red, respectively.